Water Air Soil Pollut (2017) 228:314
DOI 10.1007/s11270-017-3479-1

# Development of Highly Selective and Efficient Prototype Sensor for Potential Application in Environmental Mercury Pollution Monitoring

**Probir Kumar Sarkar · Animesh Halder · Nabarun Polley · Samir Kumar Pal**

Received: 10 February 2017 / Accepted: 12 July 2017


**Abstract** Mercury (Hg) is an environmental pollutant which is detrimental to the health of living beings due to the toxicity in its all oxidation states. To control mercury pollution development of low cost, efficient and highly sensitive prototype mercury sensor remains a challenge. In the present work, we have proposed a low-cost prototype device based on silver nanoparticle-impregnated poly(vinyle alcohol) (PVA-Ag-NPs) nanocomposite thin film for mercury detection. The thin film, fabricated through a facile protocol, is shown to be a fast, efficient, and selective sensor for $Hg^{2+}$ in aqueous medium with a detection limit of 10 ppb. We have utilized the aggregation and amalgamation of Ag-NPs with $Hg^{2+}$ to develop the low-cost, highly efficient and feasible prototype mercury sensor. In the presence of $Hg^{2+}$, the yellowish thin film turned into colourless due to the loss of intense surface plasmon resonance (SPR) absorption band of the silver nanoparticles (Ag-NPs) through aggregation and amalgamation with mercury. The developed sensor has high selectivity for $Hg^{2+}$ ions over a wide range of other competing heavy metal ions, generally present in water of natural sources. The sensor response is found to be linear over the $Hg^{2+}$ ion concentration regime from 10 ppb to 5 ppm. The developed sensor has shown to determine a trace $Hg^{2+}$ ions in real water samples. Finally, using the proposed technique, we have developed a simple and inexpensive prototype device for monitoring in field environmental mercury pollution.

**Keywords** Mercury pollution · Mercury sensor · Silver nanoparticles · Thin film · Amalgamation · Prototype device

## 1 Introduction

In concern to the human and ecological health impacts, mercury (Hg) and its compounds are considered as well-known toxic and environmental pollutant. Both elemental and ionic mercury can be converted into organo-mercury species (like methylmercury) by bacteria in the environment. These species can easily be bio-accumulated in the food chain and are detrimental to the health of living beings (Harris et al., 2003; Ke et al., 2014). The sources from which living organisms can be subjected to mercury exposure include water, air, soil and food (Eisler, 2003; Glass et al., 1991; Ke et al., 2014; Miller et al., 1996; Wang et al., 2008a; Wang et al., 2004). Mercury exposure has adverse effects on the cardiovascular system, heart, brain, kidney, lungs, central nervous system and immune system of human beings and animals, as well as organic mercury exposure may cause neurologic and mental disorders (Baughman, 2006; Farhadi et al., 2012; Ke et al., 2014; Tchounwou et al., 2003; Yan et al., 2014). One of the most usual and stable forms of mercury pollution is water-soluble oxidized divalent mercury ($Hg^{2+}$) ion (Butler et al., 2006;

P. K. Sarkar · A. Halder · N. Polley · S. K. Pal (✉)
Department of Chemical, Biological and Macromolecular Sciences, S. N. Bose National Centre for Basic Sciences, Block JD, Sector III, Salt Lake, Kolkata 700 106, India
e-mail: skpal@bose.res.in

Published online: 03 August 2017

Farhadi et al., 2012). Due to the potential impact of mercury ions on human health and the environment, the development of techniques for sensing and monitoring of mercury ions has become the focus of numerous studies. Among many different kinds of sensors, optical sensors have comprehensive advantages over other methods due to their versatility, specificity, sensitivity and real-time monitoring ability with fast response time (El-Safty and Shenashen, 2012; Nolan and Lippard, 2008). In the past decade, the commonly adopted techniques for mercury ion detection include atomic absorption spectrometry (AAS), atomic fluorescence spectrometry (AFS), inductive coupled plasma mass spectrometry (ICP-MS) (Ghaedi et al., 2006; Kim et al., 2012) and electrochemical methods (Wang et al., 2016). However, these methods generally involve complicated operation procedures, time-consuming and high costs, which greatly limit their practical applications for routine assay of mercury ion detection (Ma et al., 2016; Pepi et al., 2006). In recent years, a number of efforts have been devoted to design various kinds of chemosensors targeting the detection of mercury ions. Such sensors can be utilized for both qualitative and quantitative detection of mercury ions using various analytical and sophisticated instruments (Chen et al., 2011; De la Cruz-Guzman et al., 2014; Somé et al., 2016; Wallschläger et al., 2002). Although the aforementioned methods are sensitive and selective, they are having limitations in practical use due to rigorous sample preparation, and in certain cases, the methods are unstable or not functional in aqueous medium (Wan et al., 2009; Wanichacheva et al., 2014). To resolve such issues, noble metal nanoparticles (NPs) especially silver nanoparticles (Ag-NPs) and gold nanoparticles (Au-NPs) are extensively used in the past few years for highly selective, sensitive and cost-effective mercury sensor development (Borah et al., 2015; Kim et al., 2001; Li et al., 2013; Polley et al., 2016; Sugunan et al., 2005; Trieu et al., 2014). Ag-NPs have strong absorption band in the visible region due to surface plasmon resonance (SPR) bands and tunable optical properties induced by small changes in shape, size, surface nature and dielectric properties of the host media (Farhadi et al., 2012; Kar et al., 2016). Ag-NP-based sensors are relatively more efficient and sensitive compared to Au-NP-based sensors because of the (more than 100-fold) higher molar extinction coefficient in the visible region of optical spectrum (Paramelle et al., 2014; Thompson et al., 2008). Moreover, few potential problems including sensitivity, selectivity and cost have also been reported in the practical implementations of Au-NP-based mercury sensors (Annadhasan et al., 2014; Guo et al., 2013; Li et al., 2011; Wang et al., 2008a; Wang et al., 2008b). In addition, some of the Au-NP-based mercury sensors are not highly selective and suffer from cross-sensitivity toward other metal ions, particularly copper ($Cu^{2+}$), manganese ($Mn^{2+}$) and lead ($Pb^{2+}$). On the other hand, Ag-NPs in solution have been used for sensing mercury based on the reduction of the SPR extinction; selectivity would be high as such reactions do not occur with the majority of other transition metal ions. In the given context, development of a highly efficient, low-cost, sensitive and highly selective polymer thin film-based prototype sensor for rapid quantitative as well as specific analysis of $Hg^{2+}$ in environmental water samples is the motivation of the present work.

In this work, we report a highly efficient, low-cost polymer thin film-based portable sensor and prototype device capable of exhibiting a high selectivity for $Hg^{2+}$ in the background of a wide range of competing heavy metal ions. We have utilized SPR of Ag-NPs in a polymer (PVA) matrix, which forms homogeneous thin film on a glass substrate. We have also investigated that the embedding of Ag-NPs inside PVA would suppress degradation of the NPs. The sensing mechanism is found to be based on amalgamation of $Hg^{2+}$ with the NPs excluding the need for special functionalization of the NPs for the development of thin film-based mercury sensor. The possible interaction between Ag-NPs and mercury ions within the polymer matrix has been examined by transmission electron microscopic (TEM) studies. Characterization of the thin film thickness is performed by using scanning electron microscope (SEM). To the best of our knowledge, this is the first simple and inexpensive portable sensor and prototype device for $Hg^{2+}$ ion detection in environmental water samples with very high selectivity even in the presence of other relevant transition metal ions.

## 2 Materials and Methods

### 2.1 Materials

In this study, analytical grade chemicals were used as received without further purification for synthesis and sample preparation. Sodium citrate, silver nitrate ($AgNO_3$–99.99%), poly(vinyl alcohol) (MW-89000-

98,000) (PVA) and sodium borohydride ($NaBH_4$) were purchased from Sigma-Aldrich. All different metal ions, in the form of nitrate or chloride salts, were purchased from either Merck or Aldrich and used as received without further purification. The stock solutions (50 mM) of all metal ions were prepared by taking a known amount of chloride or nitrate salts in Millipore water.

## 2.2 Methods

### *2.2.1 Synthesis of Silver Nanoparticles and Fabrication of Thin Films*

Citrate capped Ag-NPs were prepared in aqueous solution (pH = 6.5) by reduction of $AgNO_3$ with $NaBH_4$ (Flores et al., 2010). Briefly, first a 1-mM stock solution of sodium citrate, 5-mM stock solution of $NaBH_4$ and 5-mM stock solution of $AgNO_3$ were prepared in an aqueous medium. One millilitre aliquot of stock $AgNO_3$ solution was added to 16 mL of 1 mM aqueous sodium citrate solution under stirring condition in an ice bath at around 0 °C. Then, 150 μL of a freshly prepared 5 mM aqueous $NaBH_4$ solution was added dropwise over 5 min. The initially colourless solution gradually turned to intense yellow in colour and was stirred for 2 h and 30 min. The formation of Ag-NPs was confirmed by the SPR band at around 400 nm in aqueous media (Flores et al., 2010).

In order to fabricate the sensor film, first the aqueous PVA solution was prepared by dissolving 1.6 g PVA in 10 mL of water under stirring condition upon heating at temperature around 70 °C. Then 3 mL aliquot of stock Ag-NPs solution was added in 1 mL PVA solution at room temperature under stirring condition. The resulting mixture solution is stirred for 15 min. Now, to prepare the sensor film, first of all, we make sure the glass slide size is 4.5 cm long and 1 cm wide. The prepared glass substrates (glass slides) were cleaned using soap solution and water followed by sonication with isopropyl alcohol for 30 min and dried in a hot air oven. After that, 50 μL of the well-mixed PVA-Ag-NPs mixture solution was casted on the cleaned glass substrates and subsequently heated in a hot air oven at 100 °C for 2 h. The thin film was formed on the glass substrates by encapsulating Ag-NPs in the host polymer matrix. Thereafter, the characterization studies of the fabricated sensor films were performed for further sensing application.

### *2.2.2 Optical Studies*

Optical absorption spectra of the films were measured by using Shimadzu UV-2600 spectrophotometer. For optical absorption studies, the baseline correction with PVA polymer film without Ag-NPs on glass substrate was used as reference. We used high-resolution transmission electron microscopy (HRTEM, FEI (Technai S-Twin) with acceleration voltage of 200 kV) to characterize the particle size and detailed structural information of the NPs in the PVA-Ag-NPs composite thin film before and after possible interaction with mercury ions. For HRTEM studies, the thin film samples were prepared on carbon-coated copper grids by drop-casting of the diluted samples. In order to study the thickness of the thin film, we used Quanta FEG 250 scanning electron microscope (SEM).

### *2.2.3 Procedure for $Hg^{2+}$ Sensing Experiments*

All the sensing experiments were carried out at room temperature. The Ag-NP-impregnated polymer thin film was immersed into a beaker with Millipore water for a short period of time and taken out for the measurement of absorption spectrum of the sensor film. The spectrum was marked as initial or zero-minute spectrum for comparison study. This process has been repeated at 3-min interval consecutively for 30 min with the same sensor film. To observe the effect of $Hg^{2+}$ on the films, the beaker was filled with known amount of the aqueous mercury ion ($Hg^{2+}$) solution (required amount of mercury nitrate monohydrate ($Hg(NO_3)_2{\cdot}H_2O$) was dissolved in Millipore water to prepare aqueous mercury ion ($Hg^{2+}$) solution). Similar to the aforementioned way, the spectrum of the sensor films was monitored with 3-min interval for up to 12 min. A fresh thin film was used for each new experiment. The overall procedure is shown schematically in Scheme 1.

### *2.2.4 Procedure for $Hg^{2+}$ Sensing in Real Samples:*

Tap water samples were collected from the laboratory and used as a model of real-world water samples. The used tap water samples were analysed in a National Accreditation Board for Testing and Calibration Laboratory in the city and found no trace of mercury in the samples. All the collected samples were filtered using 0.22 μm pore size nylon disk and spiked with mercury at different concentration levels by dissolving required

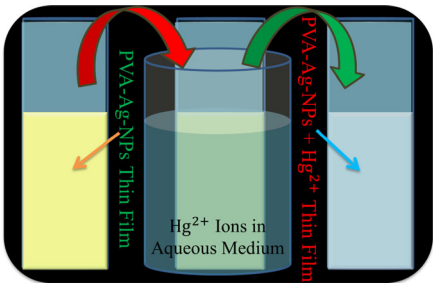


**Scheme 1** The experimental procedure and the effect of mercury ($Hg^{2+}$) ions on the silver nanoparticles (Ag-NPs) are shown schematically

amount of mercury nitrate monohydrate ($Hg(NO_3)_2{\cdot}H_2O$) salt. Final concentrations of mercury ions in the spiked tap water samples were 500 ppb, 1 ppm, 5 ppm and 10 ppm. For sensing, mercury contamination of the spiked tap water samples were measured as described earlier using our developed sensor and a correlation was traced between the measured and the expected results (obtained from the calibration equation) by comparing the differential absorbance intensity with respect to the reference sample measured at zero minute.

## 3 Results and Discussion

### 3.1 Characterization of PVA-Ag-NPs Thin Film

The film was characterized by the UV–Vis spectrophotometer. The SPR spectrum of the prepared PVA-Ag-NPs thin film is shown in Fig. 1a. The observed characteristic absorbance band peaking at around 405 nm is due to SPR band of the Ag-NPs. The absorbance band of the NPs indicates the synthesized particle size is around 11 nm (Paramelle et al., 2014). The photographic image of the sensor film is shown in the inset of Fig. 1a. For further confirmation on the consistency of the sensor film, we have used electron microscopy (TEM, SEM) on the PVA-Ag-NPs thin film. Figure 1b represents the TEM image of the citrate capped Ag-NPs within the polymer matrix. The TEM images reveal that the particles are spherical in shape with almost uniform size distribution. The average diameter of the particles is found to be around 11 nm (lower inset of Fig. 1b). The crystal structure of the metal NPs is also confirmed from the fringe-distance in the HRTEM image. Upper inset of Fig. 1b shows continuous single directional lattice

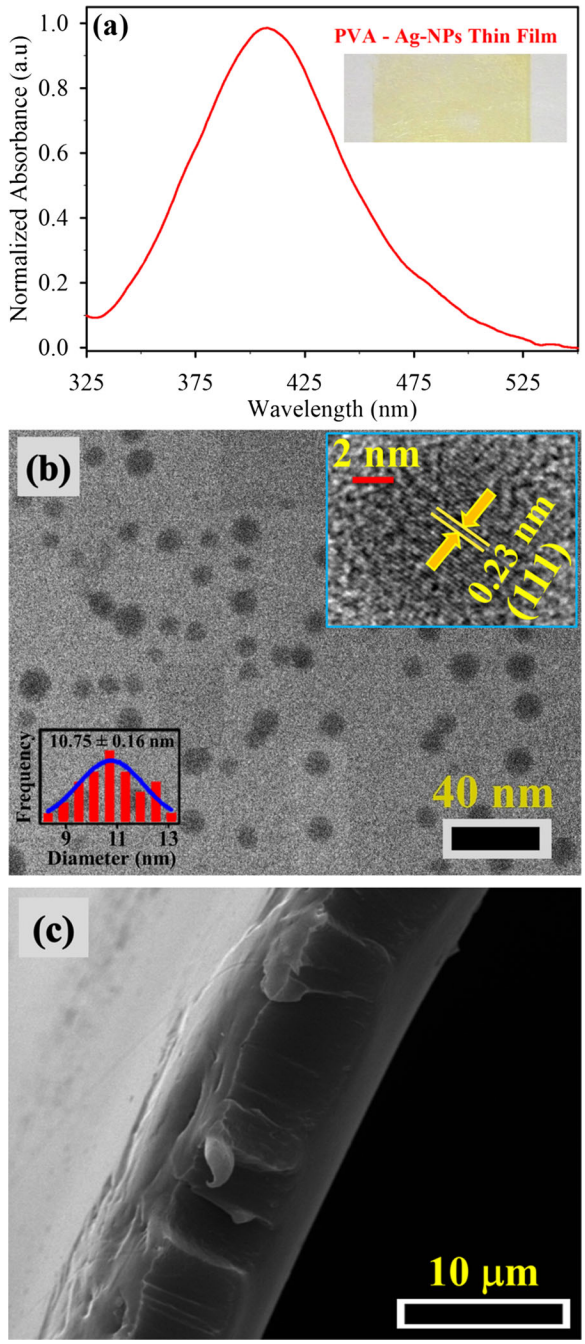


**Fig. 1** **a** Normalized UV–Vis absorbance spectrum of PVA-Ag-NPs thin film. Inset shows the image of the thin film on glass slide. **b** TEM images of PVA-Ag-NPs thin film. *Lower inset* shows the size distribution of the Ag-NPs and *upper inset* shows the high-resolution TEM (HRTEM) image of Ag-NPs. **c** SEM image of Ag-NP-impregnated PVA thin film (cross-sectional)

fringes. The measured interplanar distance of the fringes (~0.23 nm) corresponds to Ag [111] lattice planes

(Rodriguez-Leon et al., 2013). Figure 1c presents the SEM image of the Ag-NP-impregnated PVA thin film (cross-sectional) revealing average thickness of the sensor film to be around 12–13 μm.

### 3.2 Sensing Mechanism and Sensitivity Studies for $Hg^{2+}$ Detection

In order to understand how the SPR band of the nanoparticle is affected by the metal $Hg^{2+}$ ions, a control study on the prepared thin film was performed. The absorbance spectrum of the wet sensor film remains constant for more than 30 min (Fig. 2a), demonstrating that even though the polymer swells in the aqueous medium, there was absolutely no leaching of Ag-NPs into the wetting medium. Our observation is consistent with the reported literature on the Ag-NP-impregnated PVA thin film (Ramesh and Radhakrishnan, 2011). In order to measure the influence of aqueous mercury solutions on the sensor films, the SPR spectra of the films were recorded before and after introducing $Hg^{2+}$ aqueous solutions with known concentrations. The spectra for a selected set of concentrations are shown in Fig. 2. As shown in Fig. 2b, c the spectra show small but definite and reproducible decrease in absorbance within a few minutes, even at the lowest $Hg^{2+}$ concentration of 10 ppb. However, for higher concentrations of $Hg^{2+}$ ions like 500 ppb, 1 ppm and 2 ppm (shown in Fig. 2d–f), the spectra show significant change within 3 min. In addition to the decrease in intensity, the SPR peak undergoes a blue shift which becomes prominent at higher $Hg^{2+}$ concentrations (Fig. 2g–j). The relative change in absorbance with respect to zero-minute spectrum with different time in presence of various concentrations of mercury ions is shown in Fig. 3a. Event at $Hg^{2+}$ concentrations below 100 ppb, a small but gradual temporal change in the absorbance with respect to initial spectrum is evident. Although the sensitivity of the sensor increased with incubation time, for sensitivity calibration, 3 min of incubation time was chosen in our study as the changes in the absorbance in all the mercury concentrations in the time window were found to be reasonable. The effect of pH on the sensing was also investigated. We observed that the SPR absorbance of as-prepared sensor film was weaker at acidic or basic conditions compared to that in pH = 6.5. At acidic or basic conditions, the increased $H^+$ and $OH^-$ in the medium probably interact with the NPs and reduce stability of the SPR of Ag-NPs, which plays significant role in the sensing mechanism. The advantage of our sensor is that the as-prepared film exhibits the highest sensitivity at the ground water's natural pH level (pH = 6.5) revealing the possibility of the potential use of the sensor for testing ground water as is.

Figure 3b demonstrates that for all over the concentration (10 ppb–20 ppm) of $Hg^{2+}$ ions, as-prepared sensor film follows non-linearity by eq. $Y = X / (10.63 + 1.4 \times X - 2.66 \times \sqrt{X})$ with 3-min incubation time, where Y is the differential absorbance ($I_0 - I$), X is the $Hg^{2+}$ ion concentration (in ppm) and $I_0$ and I are the absorbances at 405 nm of the sensor film at 0 and 3 min, respectively. However, the inset of Fig. 3b exhibits that the differential absorbance ($I_0 - I$) and $Hg^{2+}$ ion concentration is in excellent linear correlation ($Y = 0.09 \times X + 0.014$,with correlation coefficient = 0.998) over the range 10 ppb to 5 ppm. Thus, the 3-min incubation time can be considered as sufficient duration for $Hg^{2+}$ detection in aqueous media with the lower detection limit of 10 ppb. We also observed that longer incubation time of the sensor with the test sample increased the sensitivity where 10 and 100 ppb could be distinguished confidently (Fig. 2b, c). Therefore, for longer incubation time, the lower detection limit of the sensor can be reduced to lower than 10 ppb.

In order to get insights into the reaction mechanisms of $Hg^{2+}$ sensing, further experimental results are presented in Fig. 4. Figure 4a shows decrease in absorbance at 405 nm as well as blue shift of SPR band in presence of $Hg^{2+}$ ions. The blue shift of the SPR band might be due to the formation of amalgamation at the surface of Ag-NPs (incomplete amalgamation) effectively reducing the size of the NPs. It has to be noted that complete amalgamation would abolish the SPR of Ag-NPs and subsequently induce agglomeration in order to form bigger-sized Ag-Hg alloy particles. To understand the above phenomena, TEM and EDAX spectra of the thin film were studied before and after immerging in the aqueous mercury ion solution. As shown in EDAX study, before immerging in the aqueous mercury solution, the thin film was completely free from mercury (inset of the Fig. 4a) and no aggregation was found among the NPs (Fig. 1b). However, after immerging the thin film in the aqueous mercury ion solution, TEM studies (Fig. 4b) confirmed increase of sizes of the observed NPs. Inclusion of Hg in the NPs is evident from EDAX spectrum as shown in the inset of the Fig. 4b. Our observation is consistent with the reported literature (Li et al., 2015; Polley et al., 2016; Ramesh and Radhakrishnan, 2011; Rex et al., 2006; Sarkar et al.,

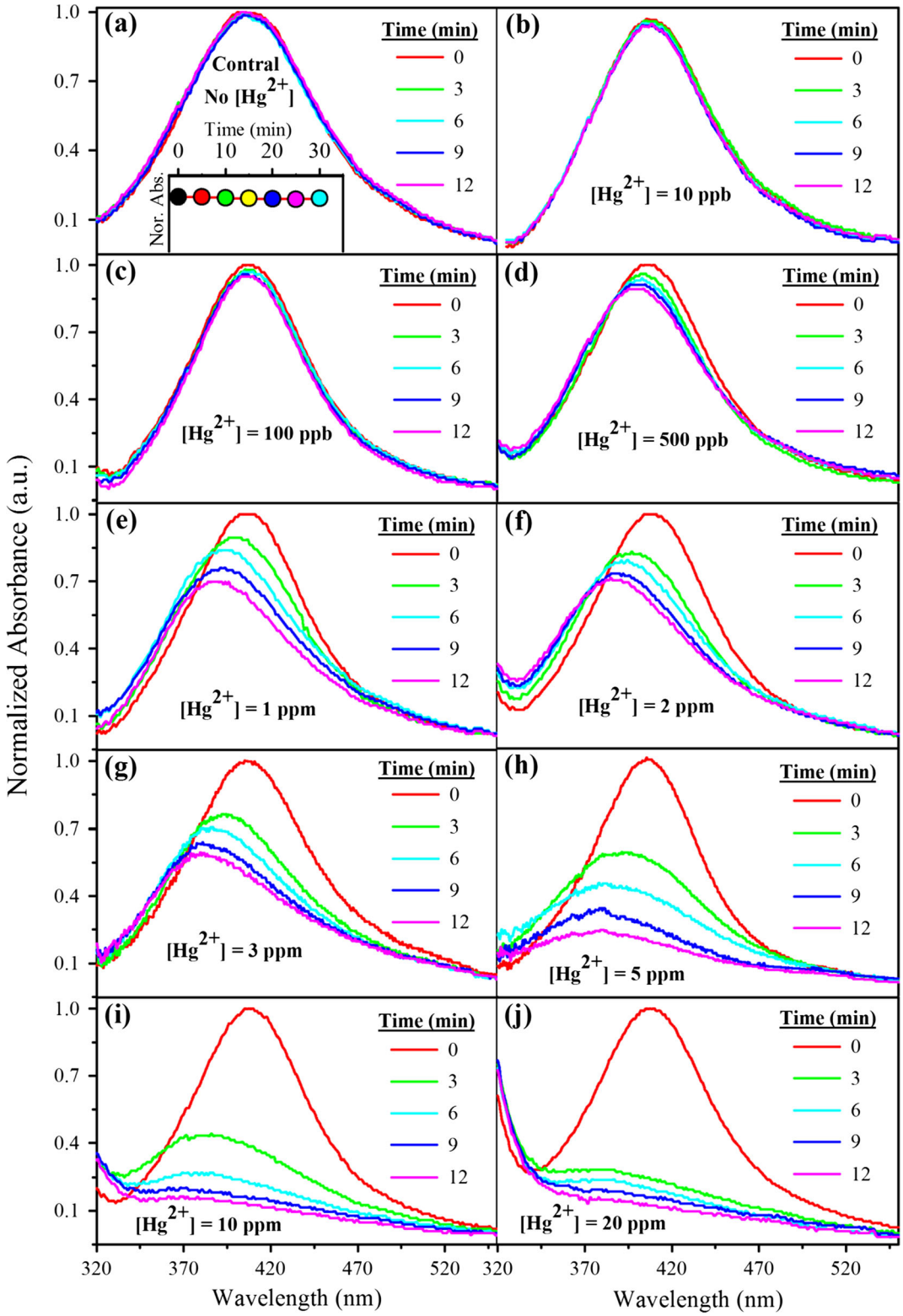


**Fig. 2** Temporal variations of the SPR spectra of PVA-Ag-NPs thin films immersed in aqueous solutions (pH = 6.5) with different concentrations of $Hg^{2+}$ ions are shown in the panels (a-j). **a** shows the variation of SPR in longer time window at $[Hg^{2+}]$ = 0 ppb. Absorbance at zero time is normalized to 1.0 in each case

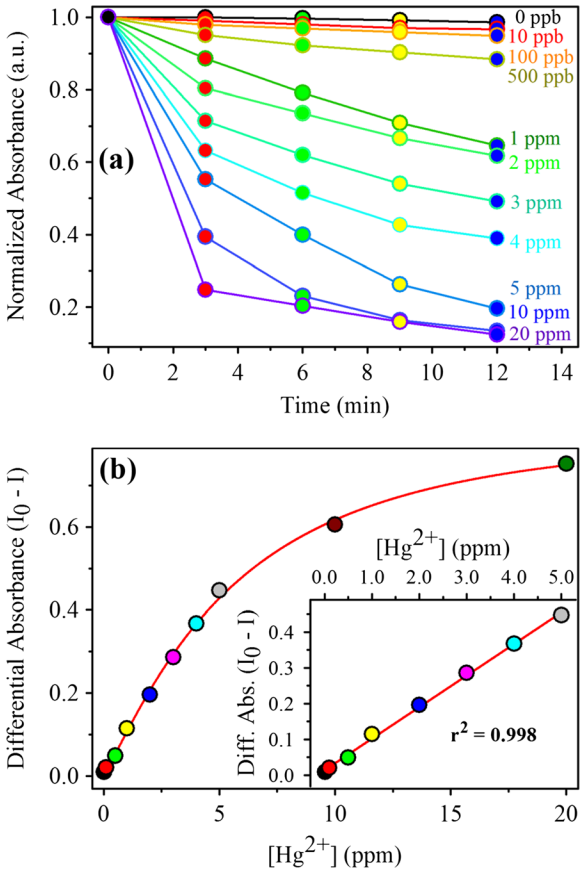


**Fig. 3** **a** Relative change in absorbance of the thin films as a function of time for different concentrations of $Hg^{2+}$ ions in aqueous medium. **b** The plot of differential absorbance of the thin films at 405 nm with $Hg^{2+}$ ions concentration. Inset shows the linear response of the sensor with [$Hg^{2+}$] from 10 ppb to 5 ppm

2016; Wang et al., 2010; Wu et al., 2012). The amalgam formed at the surface of the silver nanoparticles within the polymer matrix by reduction of $Hg^{2+}$ ions (Henglein and Brancewicz, 1997; Katsikas et al., 1996; Ramesh and Radhakrishnan, 2011). The amalgamation is unavoidable only in the presence of $Hg^{2+}$ ions because the reduction of $Hg^{2+}$ (to Hg) is most facile by Ag-NPs due to the equivalent redox potential of $Hg^{2+}$ (to Hg) ($E^0$ = 0.85 V) and Ag-NPs (to $Ag^{+1}$) ($E^0$ = 0.80 V) (Ramesh and Radhakrishnan, 2011; Ravi et al., 2013). The amalgamated/aggregated Ag-NPs lose SPR band (decrease in absorbance) and increase the particles size within the sensor film.

### 3.3 Selectivity Studies

From our earlier studies, it is evident that the Ag-NP-impregnated sensor thin film acts as an efficient mercury sensor through amalgamation/aggregation of the NPs within the polymer matrix. Now, to investigate the selectivity of the developed sensor, we have studied the interference of other metal ions including $Cu^{2+}$, $Cd^{2+}$, $Mg^{2+}$, $Co^{2+}$, $Na^{+}$, $Ca^{2+}$, $K^{+}$, $Zn^{2+}$, $Ni^{2+}$, $Pb^{2+}$, $Fe^{3+}$, and $Ag^{+}$ in the detection ability of the sensor under the same experimental condition. The changes in absorbance at 405 nm of the sensor films after the interaction (interaction time 12 min) with different metal ions and mixture of all metal ions (including $Hg^{2+}$ and excluding $Hg^{2+}$) are presented in Fig. 5a with a 5% error bar. The results

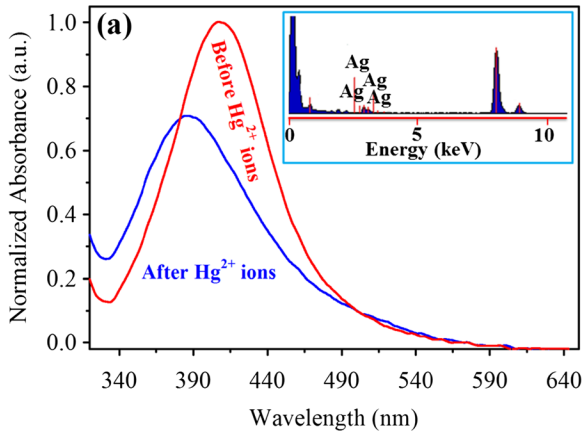


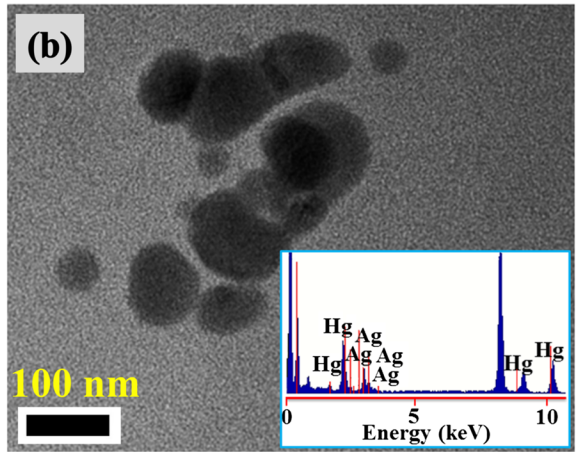


**Fig. 4** **a** Normalized UV–Vis absorbance spectrum of PVA-Ag-NPs thin film, before and after immersed in aqueous solutions of $Hg^{2+}$ ions. Inset shows the EDAX spectra of the thin film before interaction with $Hg^{2+}$ ions. **b** TEM image of the thin film after interaction with $Hg^{2+}$ ions. Inset shows the EDAX spectra of the thin film after interaction with $Hg^{2+}$ ions

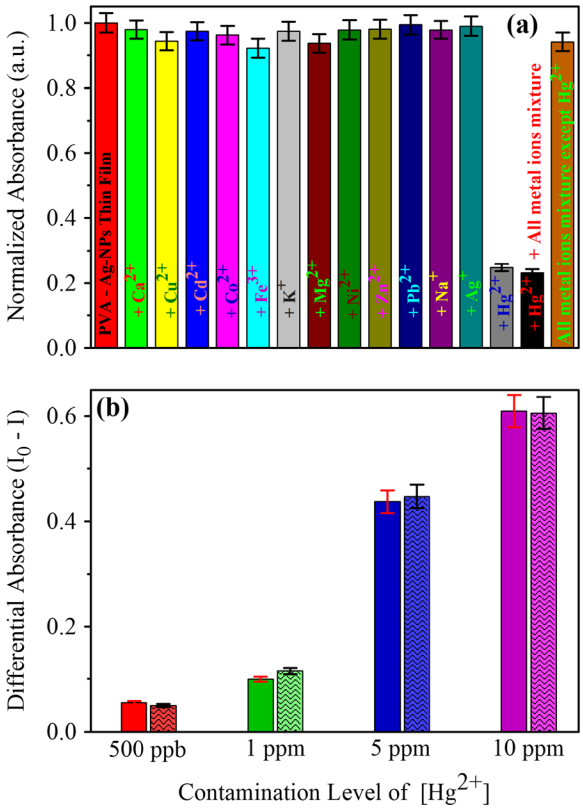


**Fig. 5** **a** Normalized UV–Vis absorbance spectra of the thin films in the presence of various metal ions, monitored at 405 nm. **b** Response of the sensor with $Hg^{2+}$ ion-contaminated real water samples and comparison of measured values (*zig-zag bars*) with expected values (*solid bars*)

demonstrate that all of those relevant metal ions (except mercury ions) and mixture of all metal ions (excluding $Hg^{2+}$) have no significant effect on the sensor thin films' optical response (Fig. 5a). The selectivity studies clearly indicate that the amalgamation/aggregation phenomenon is only evident in the presence of $Hg^{2+}$ ions because the reduction of $Hg^{2+}$ (to Hg) is most facile by Ag-NPs due to the equivalent redox potential of $Hg^{2+}$ and Ag-NPs (Ramesh and Radhakrishnan, 2011; Ravi et al., 2013). Our observation indicates that the proposed sensor has potential in real applications for monitoring environmental mercury ions in aqueous medium without any interference from other relevant metal ions.

### 3.4 Determination of $Hg^{2+}$ Ions in Real Samples

Potential application of the proposed technique was evaluated for determination of mercury ions in real samples. Laboratory tap water sample was taken for this experiment. As the collected environmental water sample was not fully purified, the metal ions are expected to be present in significant amount. The test report of the tap water from a National Accreditation Board for Testing and Calibration Laboratories test centre is as follows. *Escherichia coli*, MPN/100 ml—Nil, total hardness ($CaCO_3$)—73.2 mg/L, sulphate—26.2 mg/L, nitrate—1.6 mg/L, iron—0.04 mg/L, arsenic—0.005 mg/L, fluoride—0.194 mg/L, chlorine—17.71 mg/L, lead—0.002 mg/L, calcium—27.0 mg/L. So, it is highly challenging to detect $Hg^{2+}$ in such environmental water sample. From the experimental data, it is found that the tap water sample is free from $Hg^{2+}$ ions. Figure 5b shows that our developed sensor is capable of detecting mercury contamination in real-world samples. The obtained concentration of $Hg^{2+}$ ions from the calibration curve (calculated) and spiked values (expected) are within the 5% error range (for details of the experimental procedure see experimental section). The results are summarized in Table 1 and show good agreement with the expected values. It is also observed from Table 1 that the recoveries of $Hg^{2+}$ at different concentration levels (ratio between measured and expected values) are in between

**Table 1** Determination of $Hg^{2+}$ ions in real water samples using the proposed method

| Samples | Detection of $Hg^{2+}$ ions | Spiked $Hg^{2+}$ (ppm) | Measured $Hg^{2+}$ (ppm) | | Recovery(%)[b] | RSD(%)[c] |
|---|---|---|---|---|---|---|
| | | | Mean | SD[a] | | |
| Tap water 1 | Not detected | 0.5 | 0.49 | 0.010 | 98.0 | 2.04 |
| Tap water 2 | Not detected | 1.0 | 1.03 | 0.025 | 103.0 | 2.45 |
| Tap water 3 | Not detected | 5.0 | 5.19 | 0.055 | 103.8 | 1.06 |
| Tap water 4 | Not detected | 10.0 | 9.89 | 0.090 | 98.9 | 0.91 |

[a] *SD* standard deviation

[b] Recovery(%) = 100×(concentration found/ concentration added)

[c] RSD(%) = Relative standard deviation of three determination = Coefficient of variation´100

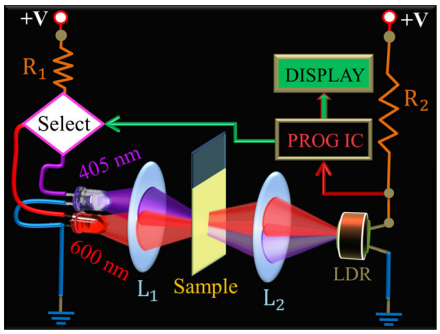


**Scheme 2** The block diagram representation of the developed prototype device for potential application in environmental mercury pollution monitoring is shown schematically

98.0 and 103.8%; the RSDs are in between 0.91 and 2.45%. It is evident from our studies that the developed thin film sensor has extremely high potential for the sensing of $Hg^{2+}$ ions in environmental water samples.

### 3.5 Development of the Prototype Device

Our studies confirmed that the developed technique has high potential application in environmental mercury pollution monitoring in the real-world water samples. By using the technique, we have developed a simple and inexpensive prototype device for monitoring in-field environmental mercury pollution. The basic block diagram of the designed prototype device is shown in Scheme 2. Here, we have used commonly available two light-emitting diodes (LEDs) with irradiance in the visible region of the electromagnetic spectrum as light sources. The violet irradiance of the LED with wavelength of 405 nm is complementary of the absorbance spectrum peak of the developed sensor thin film. The red LED with wavelength of 600 nm is used for baseline correction (reference). The lenses are used to focus the light on the sample and the LDR (light dependent resistor). Finally, the programmable IC (integrated circuit) which is connected to a digital display is used to convert the LDR signal to digital value. We will present the detailed instrumentation and the validation of the designed portable device for a statistically significant number of real-world water samples in our future work.

## 4 Conclusion

In summary, the present study illustrates the design of a simple and inexpensive prototype sensor based on silver nanoparticle-impregnated poly(vinyle alcohol) nanocomposite thin film for mercury detection. The thin film fabricated through a facile protocol is shown to be a fast, efficient and selective sensor for $Hg^{2+}$ in aqueous medium. The study demonstrates the unique potential of Ag-NPs in mercury ion sensing application followed by the reduction and blue shift of the SPR spectrum upon interaction with mercury, enhancing the selectivity of the detection, through amalgamation/aggregation process. The developed sensor is highly selective toward $Hg^{2+}$ ions, even in the presence of other metal ions generally present in water of natural sources. The sensor response exhibits excellent linear correlation with $Hg^{2+}$ ions concentration over the range 10 ppb to 5 ppm. The developed sensor has potential applications in monitoring trace $Hg^{2+}$ ions in real-world water samples. We have also developed a simple, inexpensive and feasible prototype device using the proposed technique for potential application in environmental mercury pollution monitoring.

**Acknowledgements** P. K. Sarkar is thankful to UGC (India) for providing the fellowship under UGC-RGNF scheme and N. Polley acknowledges DST (India) for INSPIRE Fellowship. We are thankful to DST (India) for Financial Grants DST-TM-SERI-FR-117, EMR/2016/004698 and DAE (India) for Financial Grant 2013/37P/73/BRNS.

## References

Annadhasan, M., Muthukumarasamyvel, T., Sankar Babu, V. R., & Rajendiran, N. (2014). 'Green synthesized silver and gold nanoparticles for colorimetric detection of Hg2+, Pb2+, and Mn2+ in aqueous medium', ACS sustain. *Chemical Engineer, 2*, 887–896.

Baughman, T. A. (2006). Elemental mercury spills. *Environmental Health Perspectives, 114*, 147–152.

Borah, S. B. D., Bora, T., Baruah, S., & Dutta, J. (2015). Heavy metal ion sensing in water using surface plasmon resonance of metallic nanostructures. *Groundwater for Sustainable Development, 1*, 1–11.

Butler, O. T., Cook, J. M., Harrington, C. F., Hill, S. J., Rieuwerts, J., & Miles, D. L. (2006). Atomic spectrometry update. Environmental analysis. *Journal of Analytical Atomic Spectrometry, 21*, 217–243.

Chen, L., Yang, L., Li, H., Gao, Y., Deng, D., Wu, Y., & Ma, L.-j. (2011). Tridentate lysine-based fluorescent sensor for Hg (II) in aqueous solution. *Inorganic Chemistry, 50*, 10028–10032.

De la Cruz-Guzman, M., Aguilar-Aguilar, A., Hernandez-Adame, L., Bañuelos-Frias, A., Medellín-Rodríguez, F. J., & Palestino, G. (2014). A turn-on fluorescent solid-sensor for Hg (II) detection. *Nanoscale Research Letters, 9*, 1.

Eisler, R. (2003). Health risks of gold miners: a synoptic review. *Environmental Geochemistry and Health, 25*, 325–345.

El-Safty, S. A., & Shenashen, M. (2012). Mercury-ion optical sensors. *Trends in Analytical Chemistry, 38*, 98–115.

Farhadi, K., Forough, M., Molaei, R., Hajizadeh, S., & Rafipour, A. (2012). Highly selective Hg2+ colorimetric sensor using green synthesized and unmodified silver nanoparticles. *Sensors and Actuators B: Chemical, 161*, 880–885.

Flores, C. Y., Diaz, C., Rubert, A., Benítez, G. A., Moreno, M. S., Fernández Lorenzo de Mele, M. A., Salvarezza, R. C., Schilardi, P. L., & Vericat, C. (2010). Spontaneous adsorption of silver nanoparticles on Ti/TiO2 surfaces. Antibacterial effect on Pseudomonas aeruginosa. *Journal of Colloid and Interface Science, 350*, 402–408.

Ghaedi, M., Reza Fathi, M., Shokrollahi, A., & Shajarat, F. (2006). Highly selective and sensitive preconcentration of mercury ion and determination by cold vapor atomic absorption spectroscopy. *Analytical Letters, 39*, 1171–1185.

Glass, G. E., Sorensen, J. A., Schmidt, K. W., Rapp, G. R., Yap, D., & Fraser, D. (1991). Mercury deposition and sources for the upper great lakes region. *Water, Air, and Soil Pollution, 56*, 235–249.

Guo, L., Xu, Y., Ferhan, A. R., Chen, G., & Kim, D.-H. (2013). Oriented gold nanoparticle aggregation for colorimetric sensors with surprisingly high analytical figures of merit. *Journal of the American Chemical Society, 135*, 12338–12345.

Harris, H. H., Pickering, I. J., & George, G. N. (2003). The chemical form of mercury in fish. *Science, 301*, 1203–1203.

Henglein, A., & Brancewicz, C. (1997). Absorption spectra and reactions of colloidal bimetallic nanoparticles containing mercury. *Chemistry of Materials, 9*, 2164–2167.

Kar, P., Maji, T. K., Sarkar, P. K., Sardar, S., & Pal, S. K. (2016). Direct observation of electronic transition-plasmon coupling for enhanced electron injection in dye-sensitized solar cells. *RSC Advances, 6*, 98753–98760.

Katsikas, L., Gutiérrez, M., & Henglein, A. (1996). Bimetallic colloids: Silver and mercury. *The Journal of Physical Chemistry, 100*, 11203–11206.

Ke, J., Li, X., Zhao, Q., Hou, Y., & Chen, J. (2014). Ultrasensitive quantum dot fluorescence quenching assay for selective detection of mercury ions in drinking water. *Scientific Reports, 4*, 5624.

Kim, H. N., Ren, W. X., Kim, J. S., & Yoon, J. (2012). Fluorescent and colorimetric sensors for detection of lead, cadmium, and mercury ions. *Chemical Society Reviews, 41*, 3210–3244.

Kim, Y., Johnson, R. C., & Hupp, J. T. (2001). Gold nanoparticle-based sensing of "spectroscopically silent" heavy metal ions. *Nano Letters, 1*, 165–167.

Li, L., Gui, L., & Li, W. (2015). A colorimetric silver nanoparticle-based assay for Hg (II) using lysine as a particle-linking reagent. *Microchimica Acta, 182*, 1977–1981.

Li, M., Gou, H., Al-Ogaidi, I., & Wu, N. (2013). 'Nanostructured sensors for detection of heavy metals: a review', ACS sustain. *Chemical Engineer, 1*, 713–723.

Li, M., Wang, Q., Shi, X., Hornak, L. A., & Wu, N. (2011). Detection of mercury(II) by quantum dot/DNA/gold nanoparticle ensemble based nanosensor via nanometal surface energy transfer. *Analytical Chemistry, 83*, 7061–7065.

Ma, Y., Zhang, Z., Xu, Y., Ma, M., Chen, B., Wei, L., & Xiao, L. (2016). A bright carbon-dot-based fluorescent probe for selective and sensitive detection of mercury ions. *Talanta, 161*, 476–481.

Miller, J. R., Rowland, J., Lechler, P. J., Desilets, M., & Hsu, L.-C. (1996). Dispersal of mercury-contaminated sediments by geomorphic processes, Sixmile canyon, Nevada, USA: implications to site characterization and remediation of fluvial environments. *Water, Air, and Soil Pollution, 86*, 373–388.

Nolan, E. M., & Lippard, S. J. (2008). Tools and tactics for the optical detection of mercuric ion. *Chemical Reviews, 108*, 3443–3480.

Paramelle, D., Sadovoy, A., Gorelik, S., Free, P., Hobley, J., & Fernig, D. G. (2014). A rapid method to estimate the concentration of citrate capped silver nanoparticles from UV-visible light spectra. *Analyst, 139*, 4855–4861.

Pepi, M., Reniero, D., Baldi, F., & Barbieri, P. (2006). A comparison of MER::LUX whole cell biosensors and moss, a bioindicator, for estimating mercury pollution. *Water, Air, and Soil Pollution, 173*, 163–175.

Polley, N., Sarkar, P. K., Chakrabarti, S., Lemmens, P., & Pal, S. K. (2016). DNA biomaterial based fiber optic sensor: characterization and application for monitoring in situ mercury pollution. *Chemistry Select, 1*, 2916–2922.

Ramesh, G. V., & Radhakrishnan, T. P. (2011). A universal sensor for mercury (Hg, HgI, HgII) based on silver nanoparticle-embedded polymer thin film. *ACS Applied Materials & Interfaces, 3*, 988–994.

Ravi, S. S., Christena, L. R., SaiSubramanian, N., & Anthony, S. P. (2013). Green synthesized silver nanoparticles for selective colorimetric sensing of Hg2+ in aqueous solution at wide pH range. *Analyst, 138*, 4370–4377.

Rex, M., Hernandez, F. E., & Campiglia, A. D. (2006). Pushing the limits of mercury sensors with gold nanorods. *Analytical Chemistry, 78*, 445–451.

Rodriguez-Leon, E., Iniguez-Palomares, R., Navarro, R., Herrera-Urbina, R., Tanori, J., Iniguez-Palomares, C., & Maldonado, A. (2013). Synthesis of silver nanoparticles using reducing agents obtained from natural sources (Rumex Hymenosepalus extracts). *Nanoscale Research Letters, 8*, 318.

Sarkar, P. K., Polley, N., Chakrabarti, S., Lemmens, P., & Pal, S. K. (2016). Nanosurface energy transfer based highly selective and ultrasensitive "turn on" fluorescence mercury sensor. *ACS Sensors, 1*, 789–797.

Somé, I. T., Sakira, A. K., Mertens, D., Ronkart, S. N., & Kauffmann, J.-M. (2016). Determination of groundwater mercury (II) content using a disposable gold modified screen printed carbon electrode. *Talanta, 152*, 335–340.

Sugunan, A., Thanachayanont, C., Dutta, J., & Hilborn, J. G. (2005). Heavy-metal ion sensors using chitosan-capped gold nanoparticles. *Science and Technology of Advanced Materials, 6*, 335–340.

Tchounwou, P. B., Ayensu, W. K., Ninashvili, N., & Sutton, D. (2003). Review: Environmental exposure to mercury and its toxicopathologic implications for public health. *Environmental Toxicology, 18*, 149–175.

Thompson, D. G., Stokes, R. J., Martin, R. W., Lundahl, P. J., Faulds, K., & Graham, D. (2008). Synthesis of unique nanostructures with novel optical properties using oligonucleotide mixed–metal nanoparticle conjugates. *Small, 4*, 1054–1057.

Trieu, K., Heider, E. C., Brooks, S. C., Barbosa Jr., F., & Campiglia, A. D. (2014). Gold nanorods for surface Plasmon resonance detection of mercury (II) in flow injection analysis. *Talanta, 128*, 196–202.

Wallschläger, D., Kock, H. H., Schroeder, W. H., Lindberg, S. E., Ebinghaus, R., & Wilken, R.-D. (2002). Estimating gaseous mercury emissions from contaminated floodplain soils to the atmosphere with simple field measurement techniques. *Water, Air, and Soil Pollution, 135*, 39–54.

Wan, Y., Niu, W., Behof, W. J., Wang, Y., Boyle, P., & Gorman, C. B. (2009). Aminoisoquinolines as colorimetric hg 2+ sensors: the importance of molecular structure and sacrificial base. *Tetrahedron, 65*, 4293–4297.

Wang, H., Wang, Y., Jin, J., & Yang, R. (2008b). Gold nanoparticle-based colorimetric and "turn-on" fluorescent probe for mercury(II) ions in aqueous solution. *Analytical Chemistry, 80*, 9021–9028.

Wang, N., Lin, M., Dai, H., & Ma, H. (2016). Functionalized gold nanoparticles/reduced graphene oxide nanocomposites for ultrasensitive electrochemical sensing of mercury ions based on thymine–mercury–thymine structure. *Biosensors & Bioelectronics, 79*, 320–326.

Wang, Q., Kim, D., Dionysiou, D. D., Sorial, G. A., & Timberlake, D. (2004). Sources and remediation for mercury contamination in aquatic systems—a literature review. *Environmental Pollution, 131*, 323–336.

Wang, Y., Yang, F., & Yang, X. (2010). Colorimetric detection of mercury(II) ion using unmodified silver nanoparticles and mercury-specific oligonucleotides. *ACS Applied Materials & Interfaces, 2*, 339–342.

Wang, Z., Heon Lee, J. & Lu, Y. (2008a). Highly sensitive "turn-on" fluorescent sensor for Hg2+ in aqueous solution based on structure-switching DNA. *Chemical Communications*, 6005–6007.

Wanichacheva, N., Hanmeng, O., Kraithong, S., & Sukrat, K. (2014). Dual optical Hg2+−selective sensing through FRET system of fluorescein and rhodamine B fluorophores. *Journal of Photochemistry and Photobiology A, 278*, 75–81.

Wu, L. P., Zhao, H. W., Qin, Z. H., Zhao, X. Y. & Pu, W. D. (2012). Highly selective Hg (II) ion detection based on linear blue-shift of the maximum absorption wavelength of silver nanoparticles. *Journal of Analytical Methods in Chemistry*. doi:10.1155/2012/856947.

Yan, Z., Yuen, M.-F., Hu, L., Sun, P., & Lee, C.-S. (2014). Advances for the colorimetric detection of Hg2+ in aqueous solution. *RSC Advances, 4*, 48373–48388.